

Electronic Supplementary Information

Multifunctional Porous Organic Polymers Embedded with Magnetic Nanoparticles

Shanlin Qiao,^{a,b} Wei Huang,^c Ting Wang,^c Bin Du,^{*,a} Xiangning Chen,^a Abdul Hameed,^d Renqiang Yang^{*,c}

^a Beijing Key Laboratory of Agricultural Product Detection and Control of Spoilage Organisms and Pesticide Residue, Faculty of Food Science and Engineering, Beijing University of Agriculture, Beijing 102206, China.

^b Institute of Chemical Industry and Pharmaceutical Engineering, Hebei University of Science and Technology, Shijiazhuang 050000, China

^c CAS Key Laboratory of Bio-based Materials, Qingdao Institute of Bioenergy and Bioprocess Technology, Chinese Academy of Sciences, Qingdao 266101, China.

^d CAS Key Laboratory of Standardization and Measurement for Nanotechnology, National Center for Nanoscience and Technology, Beijing 100190, China.

* E-mail: bindu80@bua.edu.cn (B. D.), yangrq@qibebt.ac.cn (R. Y.)

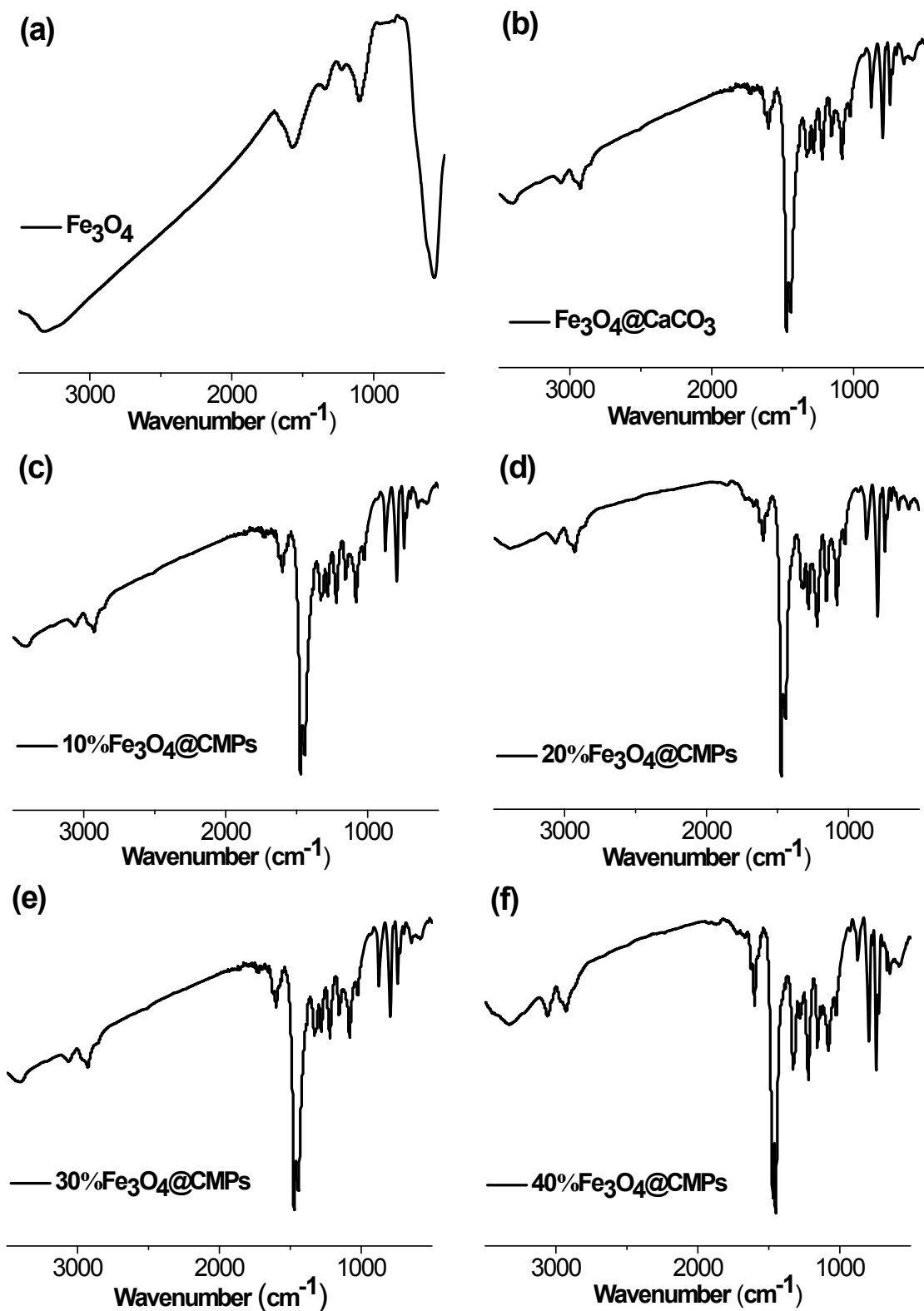


Figure S1. (a-f) FT-IR spectra of Fe_3O_4 NPs, $\text{Fe}_3\text{O}_4@\text{CaCO}_3$, and $\text{Fe}_3\text{O}_4@\text{CMPs}$.

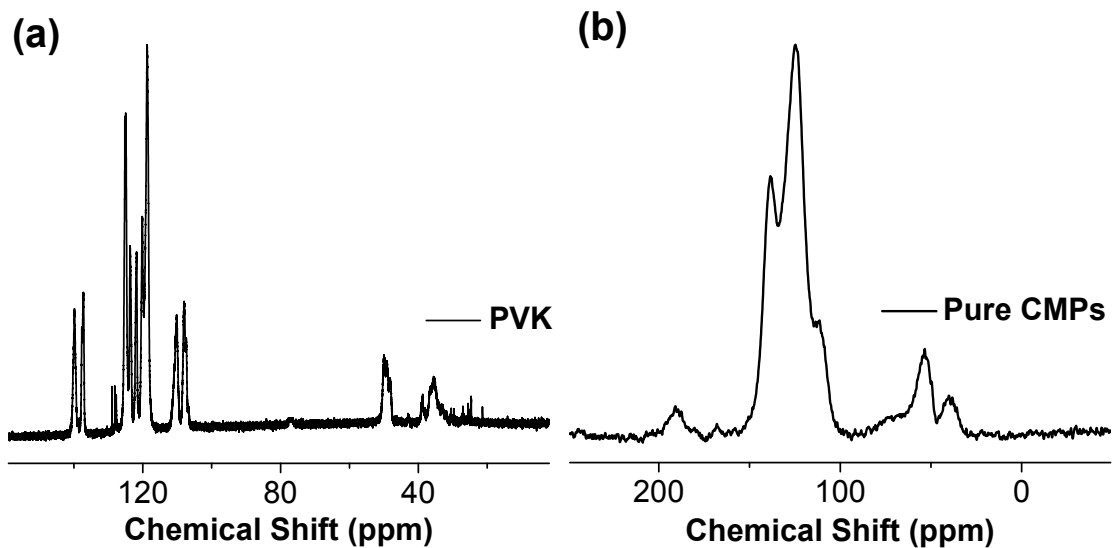


Figure S2. Solid state ^{13}C CP/MAS NMR of PVK (a) and pure CMPs (b).

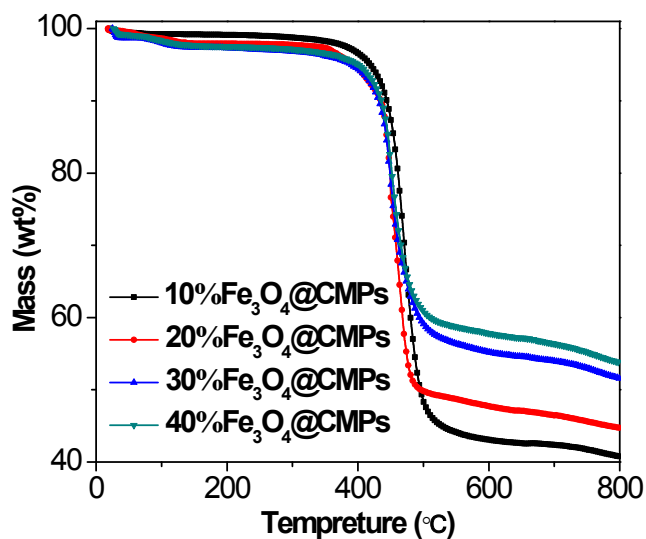


Figure S3. TGA of Fe₃O₄ NPs.

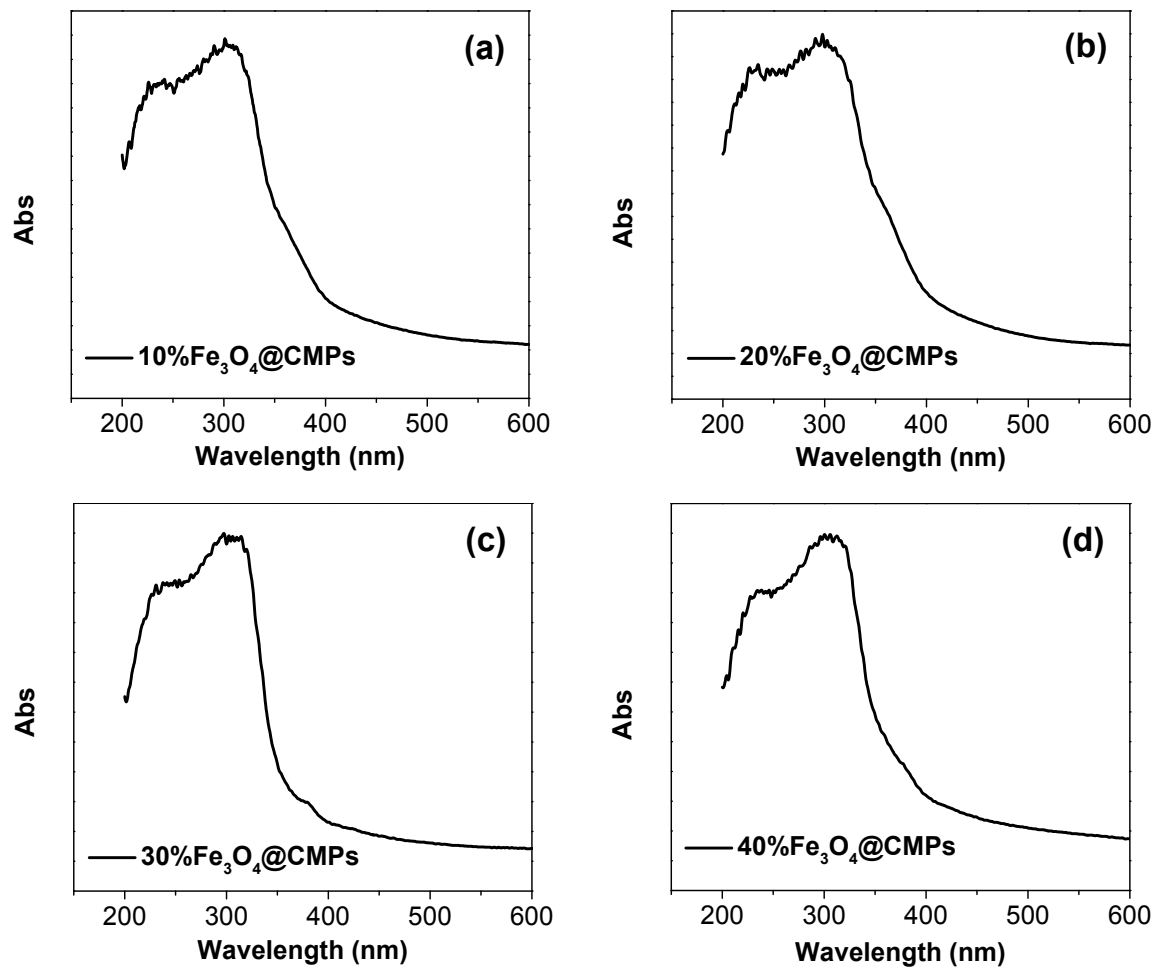


Figure S4. (a-d) UV-vis absorption spectra of $\text{Fe}_3\text{O}_4@\text{CMPs}$.

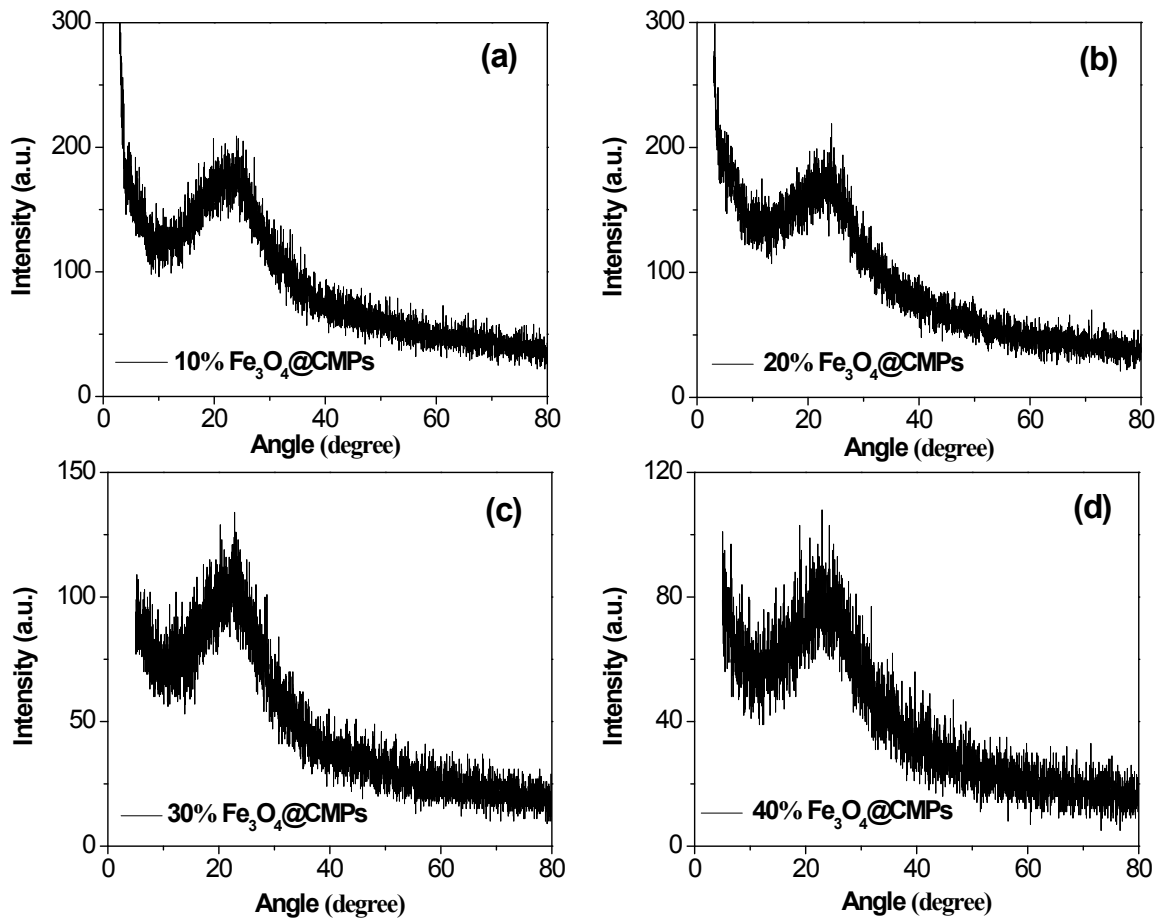


Figure S5. (a-d) Powder XRD patterns of $\text{Fe}_3\text{O}_4@\text{CMPs}$.

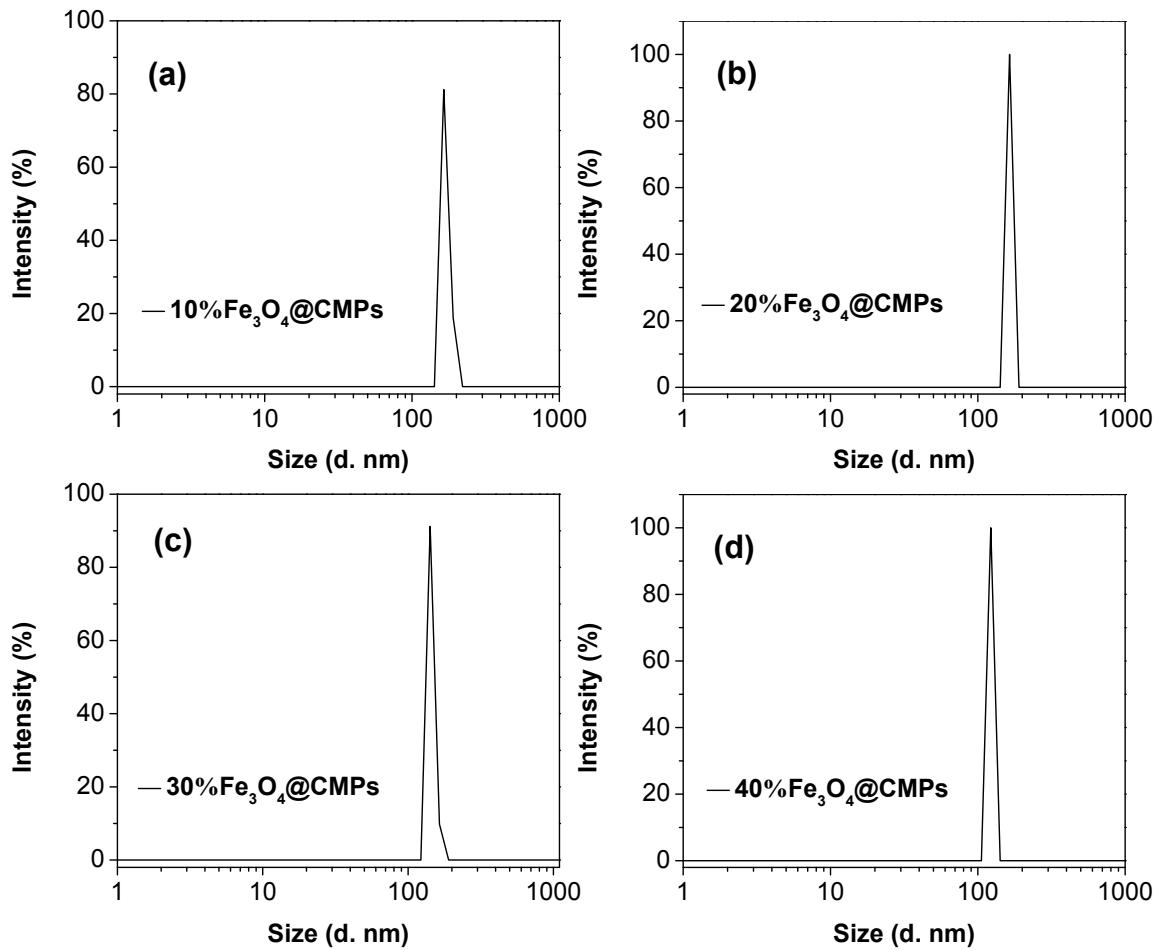


Figure S6. Particle size distribution of the Fe_3O_4 @CMPs. (a) $10\%\text{Fe}_3\text{O}_4$ @CMPs, (b) $20\%\text{Fe}_3\text{O}_4$ @CMPs, (c) $30\%\text{Fe}_3\text{O}_4$ @CMPs, and (d) $40\%\text{Fe}_3\text{O}_4$ @CMPs.

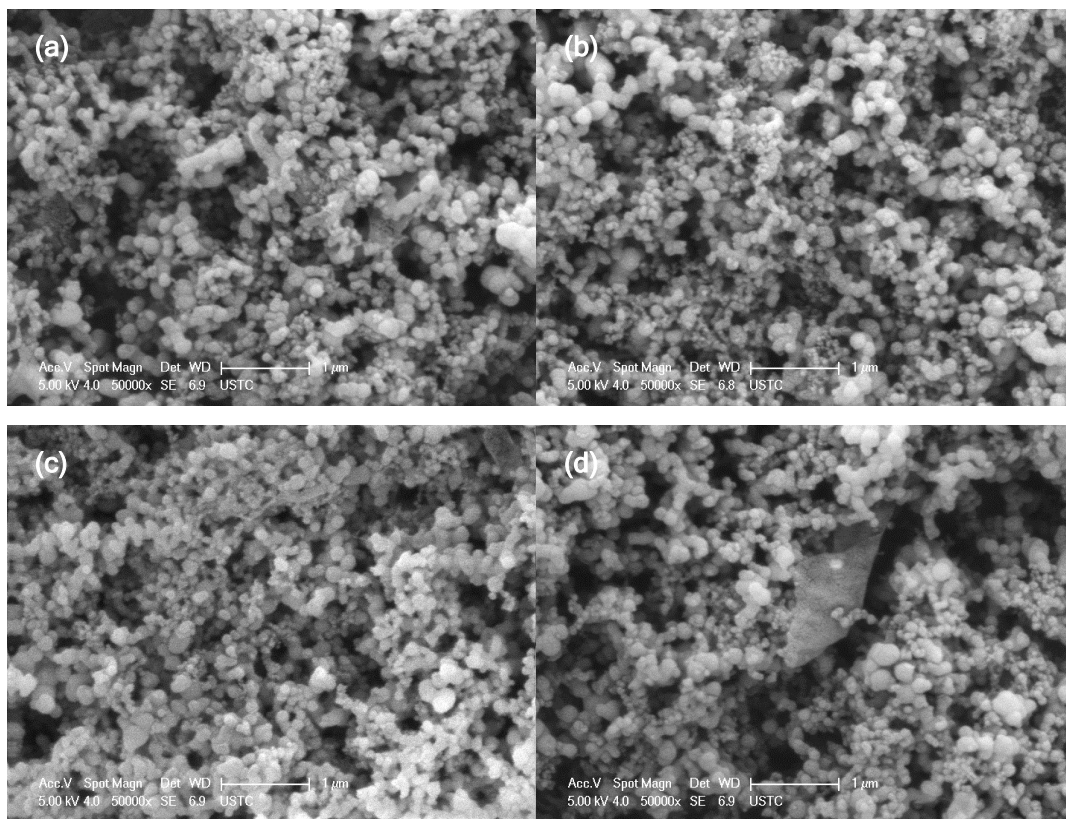


Figure S7. SEM images of Fe_3O_4 @CMPs. (a) 10% Fe_3O_4 @CMPs, (b) 20% Fe_3O_4 @CMPs, (c) 30% Fe_3O_4 @CMPs, and (d) 40% Fe_3O_4 @CMPs.

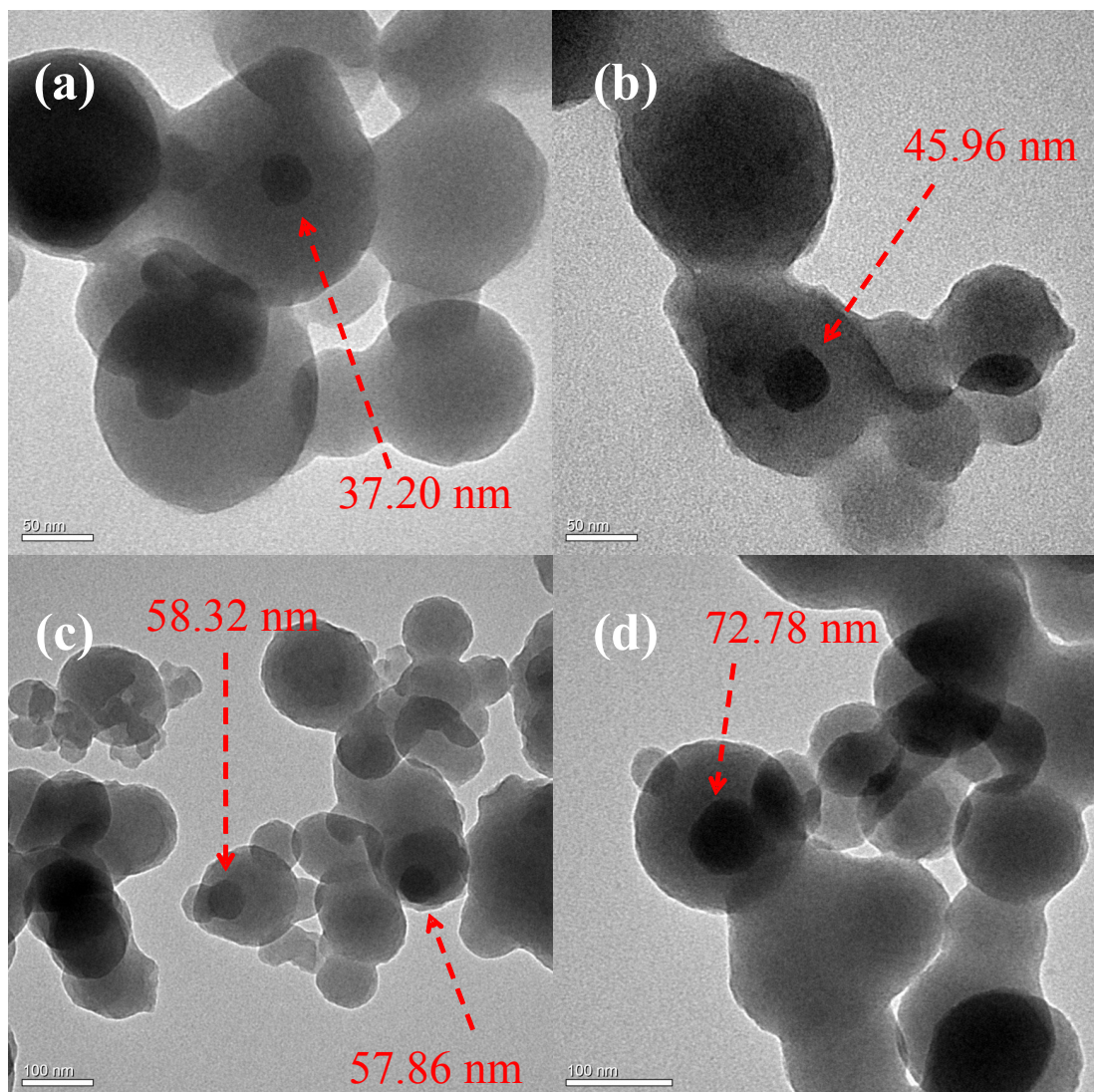


Figure S8. TEM images of Fe_3O_4 NPs core size dimension in bulk materials. (a) 10% Fe_3O_4 @CMPs, (b) 20% Fe_3O_4 @CMPs, (c) 30% Fe_3O_4 @CMPs, and (d) 40% Fe_3O_4 @CMPs.

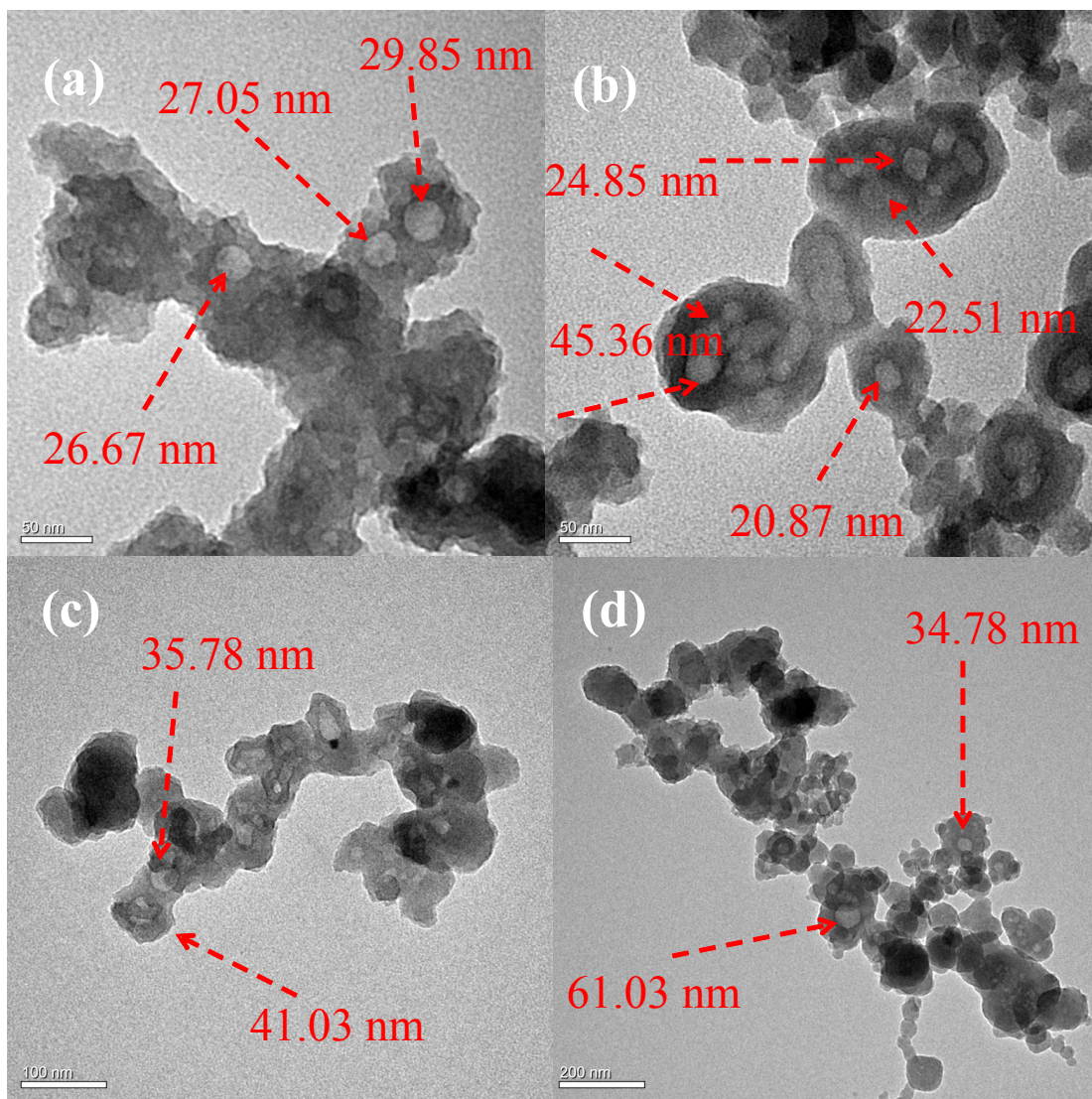


Figure S9. TEM images of holes dimension in bulk materials after etched by acetic acid solution. (a) 10%Fe₃O₄@CMPs, (b) 20%Fe₃O₄@CMPs, (c) 30%Fe₃O₄@CMPs, and (d) 40%Fe₃O₄@CMPs.

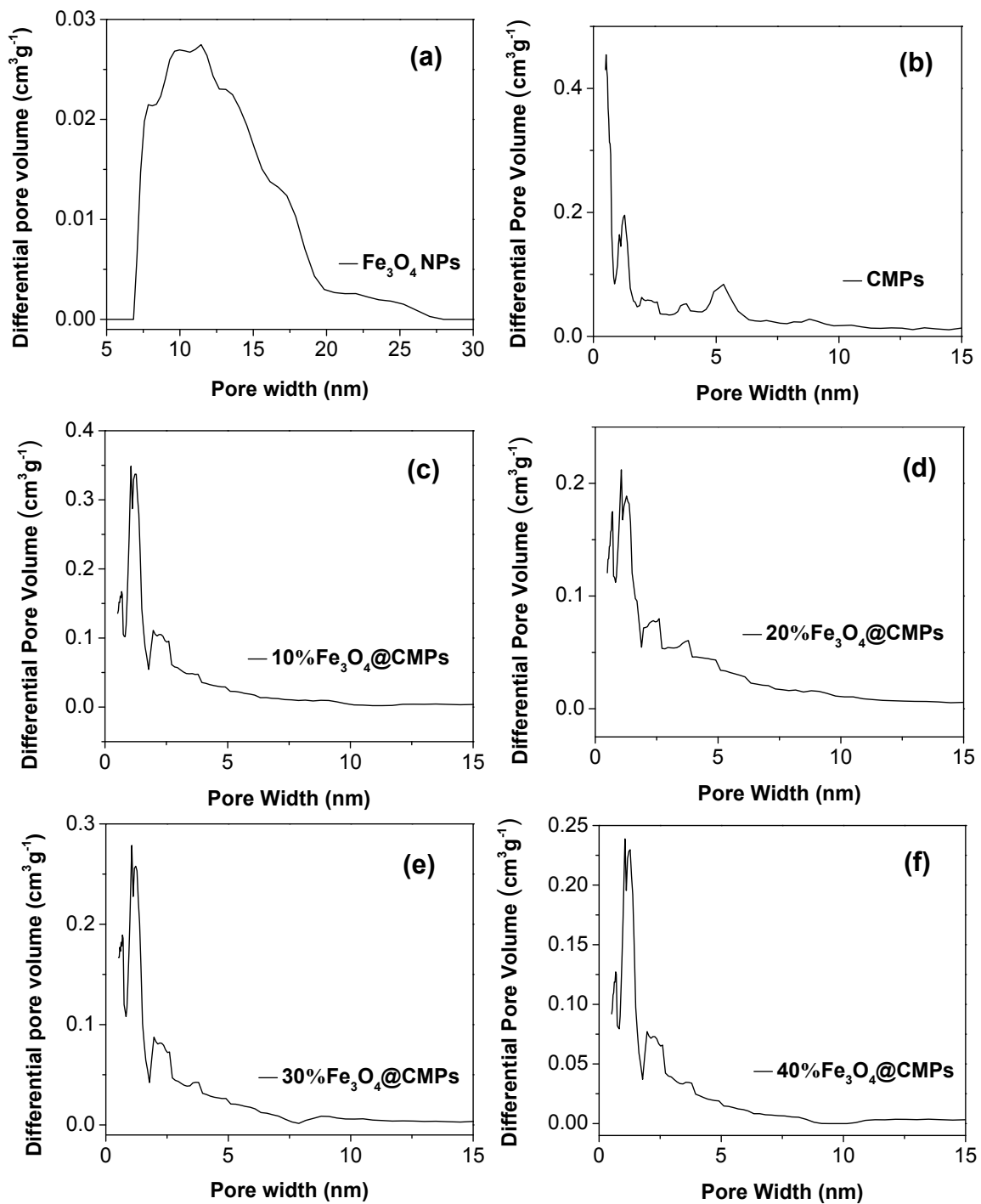


Figure S10. Pore size distribution calculated using nonlocal density functional theory

of (a) Fe_3O_4 NPs, (b) pure CMPs and (c-f) composite materials.

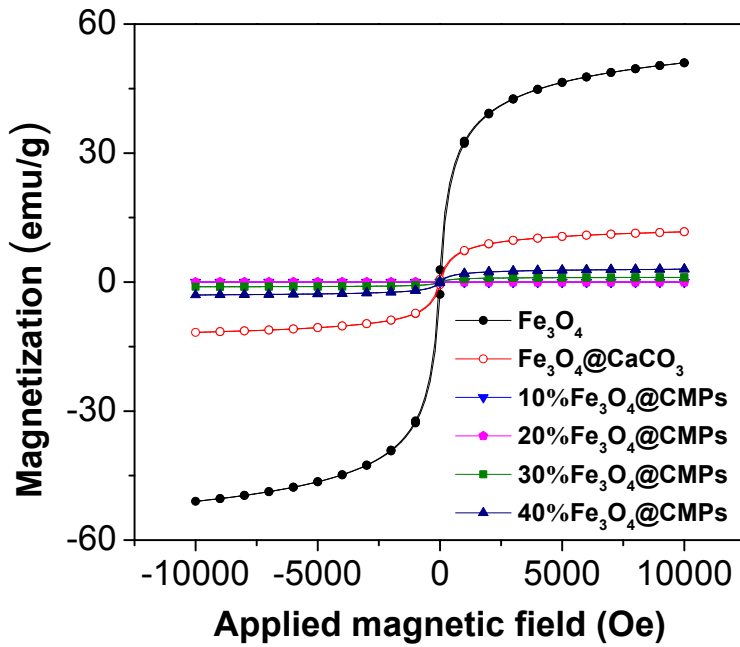


Figure S11. Hysteresis loops of Fe_3O_4 NPs, $\text{Fe}_3\text{O}_4@\text{CaCO}_3$, and $\text{Fe}_3\text{O}_4@\text{CMPs}$.

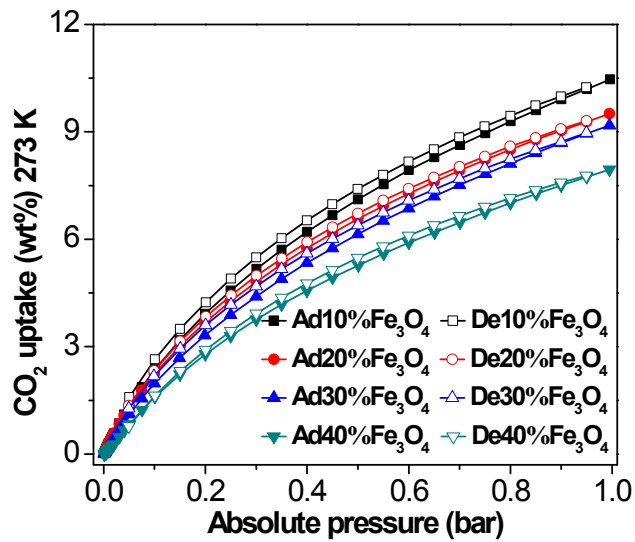


Figure S12. CO_2 adsorption and desorption isotherms at 273 K.

Table S1 Porosity properties of Fe₃O₄@CMPs compared with Fe₃O₄ and pure CMPs

	Fe ₃ O ₄	10% Fe ₃ O ₄	20% Fe ₃ O ₄	30% Fe ₃ O ₄	40% Fe ₃ O ₄	pure CMPs
BET ^a	102	735	680	636	518	878
pore volume ^b	0.26	1.43	1.24	0.95	0.78	1.00
pore size ^c	11.44	0.57	0.52	0.57	0.59	0.54

a Surface area calculated from N₂ isotherm (m² g⁻¹).b total pore volume at P/P₀ = 0.99 (cm³ g⁻¹).

c major pore size (nm).

Table S2 Adsorbing capacity of lab solvents

Solvent	10%Fe ₃ O ₄	20%Fe ₃ O ₄	30%Fe ₃ O ₄	40%Fe ₃ O ₄
	@CMPs (%)	@CMPs (%)	@CMPs (%)	@CMPs (%)
THF	1167	1136	1050	967
Ethyl acetate	1180	1152	926	857
Toluene	1170	1100	1002	906
Methanol	860	834	672	640
Hexane	500	447	390	356
Dichloromethane	1480	1400	1320	1190
Chloroform	1600	1441	1364	1285
Chlorobenzene	1298	1200	1120	1030
1,2-Dichlorobenzene	1633	1540	1480	1380